Jestr

Journal of Engineering Science and Technology Review 17 (4) (2024) 205-209

Research Article

JOURNAL OF
Engineering Science and Technology Review

www.jestr.org

SER Analysis of GFDM System over α – μ Fading Channel for 5G Wireless Applications

Lingaiah Jada* and S.Shiyamala

School of Electrical and Communication Engineering, ECE, Vel Tech Rangarajan Dr.Sagunthala R&D Institute of Science and Technology, Avadi,Chennai-600 062,Tamilnadu,India

Received 13 June 2023; Accepted 27 December 2023

Abstract

A flexible radio waveform, generalised frequency division multiplexing (GFDM) allows for significant degrees of freedom in adjusting the number of time slots, subcarriers, and pulse shaping filters. The GFDM is one of the multi-carrier techniques that has been proposed to achieve 5G requirements. Initially, this study discusses about the derivation of novel analytical expression of symbol error rate under $\alpha - \mu$ fading channel using the GFDM system. The proposed derivation includes Rayleigh, Nakagami-m, and Nakagami-q fading channels as special cases for different α and μ values. Further, a simulation test-bed has been developed in MATLAB to access the simulation results and they are in good agreement with the derived theoretical results for various simulation parameters such as different roll-off factors, modulation orders and various fading parameters.

Keywords: GFDM, SER (symbol error rate), $\alpha - \mu$ fading channel, roll-off factor, SNR.

1. Introduction

In present days, 5G systems need to have very low latency, reliability, robust high throughput, and low value of out of band (OOB) emission. Several noteworthy waveforms have been designed in the literature for this situation. Because of its desirable qualities, including minimal OOB radiation to enable dynamic spectrum access and low latency, generalized frequency division multiplexing (GFDM) is one of the top options for future wireless applications. In GFDM, majority of the subcarriers are non-orthogonal to one another, which is the key difference between it and OFDM (orthogonal frequency division multiplexing) [1]. Cyclic prefixes (CP), which consume a lot of bandwidth, are not added to each subcarrier, which is another significant benefit of GFDM. We obtain the identical at the receiver in bits as those which are broadcast by the transmitter in GFDM because just to the combination of sub carriers, one CP is added [2]. According to [3–4], the GFDM system is less complex, achieves minimal OOB, and offers a viable 5G option. The authors of [5] addressed how the adaptable technology known as GFDM circumvents the problems with 4G technology. In a nutshell, GFDM sends data in the form of data blocks made up of K sub carriers and M sub-symbols. Each sub-carrier in GFDM has a low OOB radiation pulse with a circular shape.

As discussed earlier, GFDM is a non-orthogonal and we can make it orthogonal by employing different pulse shaping filters. Additionally, as GFDM is a less complicated method, it can be accomplished by combining it with orthogonal quadrature amplitude modulation (OQAM) [6-7]. To fulfil the demands of the most recent technologies, the GFDM system uses a variety of circular pulse shaping filters addressed in [8–10].

Numerous studies have been conducted on the performance of GFDM's bit error rate (BER) in various fading channels, considering a variety of pulse shaping candidates at receiver that include zero forcing (ZF) and matched filter (MF) in [11–16]. In order to eliminate self-interference, the ZF receiver is used in performance evaluation of GFDM for time-varying Rayleigh fading channels in terms of SER. However, noise enhance factor (NEF) [5] is used to boost up SER performance to overcome loss occur due to pulse shaping filter [17]. In [14-15], SER analytical expressions are provided under several fading environments. The SER expression over AWGN channel for GFDM system with a ZF receiver is shown in [5]. Nevertheless, multiple input multiple output (MIMO), which is one of the key enabler for 5G to achieve diversity is also suitable with GFDM [21-22]

One of the most important aspects of designing a communication system is modelling a wireless channel. The $\alpha - \mu$ distribution is generalized fading and it is used in non-line of sight (NLOS) channel environments. The Rayleigh, Nakagami-m, and Nakagami-q channels can be achieved for special values of $\alpha - \mu$ [3]-[23]. The GFDM system analysis under $\alpha - \mu$ fading is not much addressed in the literature. This motivates us to derive the analytical expressions of symbol error rate using GFDM system with ZF receiver under $\alpha - \mu$ fading channel. In particular, with the help of MATLAB software simulation results are validate with the analytical formulations.

The following major contributions are added to the literature with this article;

- The novel analytical SER expression for $\alpha - \mu$ fading channel is derived and Monte-Carlo simulated test bed has developed to valid theoretical results.

*E-mail address: vtd488@veltech.edu.in
ISSN: 1791-2377
doi:10.25103/jestr.174.22

- The effect on SER is shown using the simulations for various fading parameters α and μ by fixing one parameter while varying the other.
- The GFDM system performance analysed for various roll-off factors.
- The effect of modulation order on the SER performance is studied.

The remaining four sections of the paper are structured as follows. The GFDM system model is discussed in section - 2. The innovative closed form of mathematical SER analysis under $\alpha - \mu$ fading is the subject of Section-3. Sections 4 and 5 present simulation analysis and results respectively.

2. System Model Description

2.1. Background of paper

Fig.1. depicts the GFDM transceiver. The vectorial data (**b**) provided to the encoder that convert low bit rate input to a high bit rate data stream vectors ($\boldsymbol{b_c}$). The mapper block generates a **N X 1** data vector as output (**d**). This vectorial data is fed into an *N*-element GFDM modulator as input. The total vectorial data (**d**) is divided into **K** groups and **M** data symbols;

$$d = [(d_0)^T, (d_1)^T, \dots \dots (d_{K-1})^T]^T \quad (1)$$

with

$$d_k = \left[d_{k,0}, d_{k,1}, \dots \dots d_{k,M-1}\right]^T \quad (2)$$

The term $d_{k,m}$ in eq. (2) represents the data symbol which will be passed through *k*-th sub carrier at *m*-th time slot. Later, it is multiplied with pulse shaping filter $\boldsymbol{g_{k,m}}(\boldsymbol{n})$. A GFDM block that uses **K** subcarriers, each of which has **M** data symbols, and generates **N** = **KM** samples. These sample values are filtered using a suitable transmit filter while using GFDM modulator is given as [11];

$$g_{k,m}[n] = g[(n - mk) mod N] e^{\frac{-j2\pi kn}{K}} \quad (3)$$

where $\boldsymbol{g_{k,m}}(\boldsymbol{n})$ is both time and frequency shifted of $\boldsymbol{g(n)}$. The GFDM signal $x(n)$ can be is expressed as follows given in [11];

$$x[n] = \sum_{k=0}^{K-1} \sum_{m=0}^{M-1} d_{k,m} g_{k,m}[n], \; n = 0,1 \dots \dots KM - 1 \quad (4)$$

The samples of pulse shaping filter is;

$$g_{k,m} = \left[g_{k,m}[0], g_{k,m}[1] \dots \dots g_{k,m}[MK-1]\right]^T \quad (5)$$

The eq. (4) can be shown in matrix form as [12];

$$\mathbf{x} = \boldsymbol{Ad} \quad (6)$$

Where $\boldsymbol{A}$ is GFDM matrix of size is $\boldsymbol{KM\ X\ KM}$ and it can be shown as [5];

$$A = \left[g_{0,0} \cdots g_{K-1,0} \quad g_{0,1} \cdots g_{K-1,M-1}\right] \quad (7)$$

After GFDM block, cyclic prefix (CP) of length N_{cp} and cyclic suffix (CS) of length N_{cs} are added and then it transmitted through the channel.

2.2. Channel model

After removing CP, the received signal can propagate across the wireless channel using the following model:

$$r = \boldsymbol{H}\mathrm{x} + \boldsymbol{w} \quad (8)$$

Where $\boldsymbol{H} = circ\{\tilde{h}\}$.

The GFDM signal is multiplied by the MRT coefficients and is represented mathematically as;

$$r = \sqrt{P_t} \sum_{i=0}^{N_t} h_i w_i x + w = \sqrt{P_t} h_F x + w \quad (9)$$

2.3. Reception of channel model

We have used ZF receiver as GFDM demodulator. The demodulated signal can be expressed as [5];

$$\hat{d} = \boldsymbol{B}y \quad (10)$$

Demodulation matrix is **B.**

$B_{ZF} = A^{-1}$ is the receiver demodulation matrix for ZF receiver. The self-interference is eliminated by a ZF receiver, but noise effect is increased. When using a ZF receiver, NEF (ζ)mathematical expression is [5], indicates how much the SNR value is reduced;

$$\xi = \sum_{i=0}^{MK-1} \left|[B_{ZF}]_{k,i}\right|^2 \quad (11)$$

where 'ξ' is equal for all $k = 0,1, \dots . MK - 1$. We took $\alpha - \mu$ fading channel into consideration in this article. The analysis compress to some frequently used fading channels for some values of $\alpha - \mu$.

Table 1. Representation of various fading channels for different $\alpha - \mu$ values.

$\boldsymbol{\alpha - \mu}$ **values**	**Fading Environment**
α=2 and μ=1	Rayleigh fading
α=2 and $\mu > 1$	Nakagami-μ fading
μ=1	Weibull fading

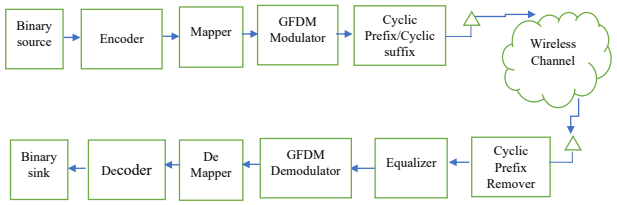

Fig. 1. GFDM Transceiver

$\alpha - \mu$ Distribution:

The $\alpha - \mu$ distribution can be used to model fading channels in the environment characterized by non-homogeneous obstacles that may be nonlinear in nature. The $\alpha - \mu$ fading also considers the received signal to be collection of clusters of multipath components.

The physical relation between resultants of received multipath clusters and fading amplitude for $\alpha - \mu$ distribution can be given as;

$$X^{\alpha,\mu} = \sum_{i=1}^{n}(I_i^2 + Q_i^2) \tag{12}$$

Where n is the number of clusters, I_i and Q_i are the resultant in-phase and quadrature phase components of $i-th$ cluster in the received signal.

3. Symbol Error Rate Analysis

This section deals with the mathematical analysis of SER expression under $\alpha-\mu$ fading channel for GFDM system. Using a ZF receiver and the QAM modulation technique, the SER performance is assessed.

1). SER Calculation in AWGN Environment

The expression for SER utilising the GFDM scheme under the AWGN is [5];

$$P_{SER,AWGN}(\gamma) = 2\left(\frac{p-1}{p}\right)erfc\left(\sqrt{\gamma}\right) - \left(\frac{p-1}{p}\right)^2 erfc^2\left(\sqrt{\gamma}\right) \tag{13}$$

Where

$$\gamma = \frac{3R_T}{2(2^m-1)}\frac{E_S}{\xi N_0} \text{ and } R_T = \frac{KM}{KM+N_{CP}+N_{CS}} \tag{14}$$

In eq. (13) and eq. (14), $p=\sqrt{2m}$, m-represents number of bits, N_{CP} , N_{Cs} are length of CP and CS respectively. K and M are number of subcarriers and data symbols. For various fading environments SER expression can be calculated using [5];

$$P_{SER} = \int_0^{\infty} P_{AWGN}(\gamma)P_{\gamma}(\gamma)d\gamma \tag{15}$$

In eq. (15), $P_{\gamma}(\gamma)$ represents the PDF of different fading channels.

2) $\alpha-\mu$ Fading Environment

In order to calculate SER expression for $\alpha-\mu$ fading, we require PDF of $\alpha-\mu$ fading. It is given in [26] as;

$$P_{\gamma}(\gamma) = \frac{\alpha\mu^{\mu}\gamma^{\frac{\alpha\mu}{2}-1}}{2\Gamma(\mu)\bar{\gamma}^{\frac{\alpha\mu}{2}}}e^{-\mu\left(\frac{\gamma}{\bar{\gamma}}\right)^{\frac{\alpha}{2}}} \tag{16}$$

where $\bar{\gamma}$ is average channel SNR.

The SER expression for $\alpha-\mu$ fading can be calculated by substituting eq.(13) and eq.(16) in eq.(15) and it obtained as;

$$P_{\alpha-\mu}(e) = 2\left(\frac{p-1}{p}\right)A\left(\bar{\gamma}_{\alpha-\mu}\right) - \left(\frac{p-1}{p}\right)^2 B\left(\bar{\gamma}_{\alpha-\mu}\right) \tag{17}$$

where $\bar{\gamma}_{\alpha-\mu}$ is equivalent SNR under $\alpha-\mu$ fading channel given by

$$\bar{\gamma}_{\alpha-\mu} = \frac{2R_T\sigma^2_{\alpha-\mu}}{\left(2^b-1\right)}\frac{E_s}{\xi N_o} \tag{18}$$

where b is number of bits per QAM symbol and $\phi=\sqrt{2^b}$.

$$R_T = \frac{NM}{NM+N_{cp}+N_{cs}} \tag{19}$$

The NEF value for ZF-receiver can be calculated as;

$$\xi = \sum_{n=0}^{NM-1}\left|\left(B_{ZF}\right)_{i,n}\right|^2 \tag{20}$$

Eq. (17) consists of two unknown values such as $A\left(\bar{\gamma}_{\alpha-\mu}\right)$ and $B\left(\bar{\gamma}_{\alpha-\mu}\right)$ which can be computed as

$$A\left(\bar{\gamma}_{\alpha,\mu}\right) = 1 - \frac{1}{2\sqrt{\pi}}\frac{\alpha\mu^{\mu}\sqrt{k}\,(l)^{\alpha\mu/2}}{\Gamma(\mu)\bar{\gamma}^{\frac{\alpha\mu}{2}}(2\pi)^{\frac{l+k-2}{2}}}G^{k+l,l}_{2l,k+l}\left[\frac{\mu^k l^l}{k^k\bar{\gamma}^{\frac{\alpha\mu}{2}}}\middle|\begin{matrix}\Delta\left(l,\frac{1-\alpha\mu}{2}\right),\Delta\left(l,1-\frac{\alpha\mu}{2}\right)\\ \Delta(k,0),\Delta\left(l,\frac{-\alpha\mu}{2}\right)\end{matrix}\right] \tag{21}$$

$$B\left(\bar{\gamma}_{\alpha,\mu}\right) = 1 - \frac{2}{\pi}\frac{\mu^{\mu}}{\left(\bar{\gamma}\right)^{\frac{\alpha\mu}{2}}}\sum_{j=0}^{\mu-1}\sum_{i=0}^{\infty}\frac{(-1)^i\left(\bar{\gamma}\right)^{\frac{\alpha}{2}(\mu-j)}}{j!\,i!\,\mu^{\mu-j}}\frac{\sqrt{k}l^{i+\frac{\alpha j}{2}-\frac{1}{2}}}{(2\pi)^{\frac{l+k-2}{2}}}G^{k,2l}_{2l,k}\left[\frac{l^l\mu^k}{\bar{\gamma}^{\frac{\alpha k}{2}}k^k}\middle|\begin{matrix}\Delta\left(l,\frac{1}{2}-i-cj\right),\Delta(l,-i-cj)\\ \Delta(k,0),\Delta\left(l,-i-cj-\frac{1}{2}\right)\end{matrix}\right] \tag{22}$$

The exact SER expression can be obtained by substituting eq. (21) and eq. (22) in eq. (17).

4. Results and Discussions

The findings of the simulation and their analysis are covered in this section. All simulations are run for 10^5 Monte-Carlo iterations with the following simulation parameters: length of CP and CS are N_{cp}=8, N_{cs}=0, K=64, M =5 and 16-QAM

The SER analysis is evaluated for various values of E_s/N_o with single antenna ($N_t=1$) and β=0.1 under $\alpha-\mu$ fading. The Fig.2 is simulated for different μ values and fixed α value (α=2). The analytical values achieved from the derived theoretical expressions is in good agreement with the Monte-Carlo simulations. It is observed that SER performance reduces with the increases in μ value. At SNR=15dB, SER values are 0.163, 0.094, 0.0688 and 0.055 for μ=1, 2, 3 and 4 respectively. It can be observed that for $\mu=1$ the curve obtained in Fig. 2 matches to that of [5]. As discussed in the Section 3, $\alpha-\mu$ distribution covers Nakagami-m as special case for α=2 and $\mu=m$. The results also confirm the same that Fig.2 is the plot for the SER performance of Nakagami-m distribution [28-30].

In Fig.3 also SER performance is investigated for different E_s/N_o values under $\alpha-\mu$ fading. This simulation is evaluated using $N_t=1$, β=0.1, and keeping one fading parameter is constant (μ=1) and varying another fading

parameter (α=2,3,5,7). This simulation is giving an exact SER response of Weibull fading with μ=1 which is discussed in [30]. We can also deduce from the Fig.3 that SER values decrease with increase in α value.

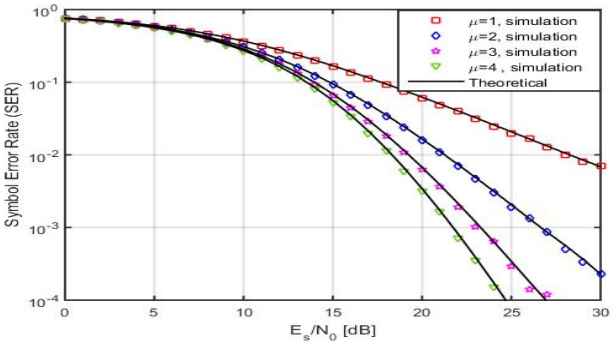

Fig. 2. SER vs E_s/N_o performance for different μ and α=2 values.

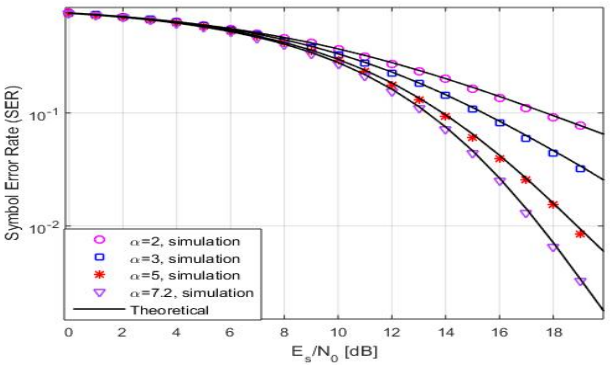

Fig. 3. SER vs E_s/N_o analysis for various values of α and μ=1.

At SNR=15dB, SER values are 0.1683, 0.117, 0.065 and 0.0462 for α= 2, 3, 5, and 7 respectively. The SER value decreases by almost 72.5%, as α value rises from α=2 to α=7, showing that fading becomes less severe as α increases. As discussed in the Section 3, $\alpha-\mu$ distribution covers Weibull as special case for α varies and $\mu=1$.

The SER performance is analysed for various β values, different SNR values (10dB, 15dB, 18dB), $\mu=3$, $\alpha=2$, and employing the 16-QAM modulation technique in Fig.4. According to the simulation, the SER value decreases from 0.286 to 0.01781 at a value of β=0.4 as SNR value grows from 10dB to 18dB. This indicates that there is an almost 95% improvement in SER with the increase in SNR. The SER value decreases at lower values of β and it rises at higher levels of β. Finally, it can be said that it is always advisable to attain less SER at lower values of β=0.1 and greater SNR values (20dB). This occurs because of rise in β value, decrease the overlap between neighbouring subcarriers, which causes a rise in NEF value (ξ) and, ultimately, a decline in SER performance is observed. It is also observed that the SER value reduces due to rise in signal power as the SNR climbed from 10dB to 18dB.

The relationship between SER and E_s/N_o is depicted in fig.5 for various roll-off factors (0.1, 0.6, and 0.9), $\mu=4$, $\alpha=2$, and employing 16-QAM modulation technique. The impact of the NEF parameter, which is important in GFDM, is also explained using Fig. 5. Because of the wider overlap of the subcarriers, which causes an increase in the NEF factor, so that we can observe noticeable change in the SER curve with the rise of roll-off factor's value. The SER values are 0.0034, 0.0074, and 0.0172 for β=0.1, 0.6, and 0.9 at SNR=20dB. The SER value lowers by 80.2% as the value of β falls from 0.9 to 0.1.

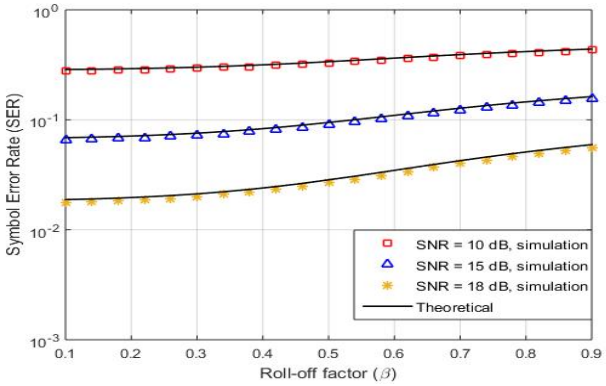

Fig. 4. SER vs roll-off factor for various SNR values.

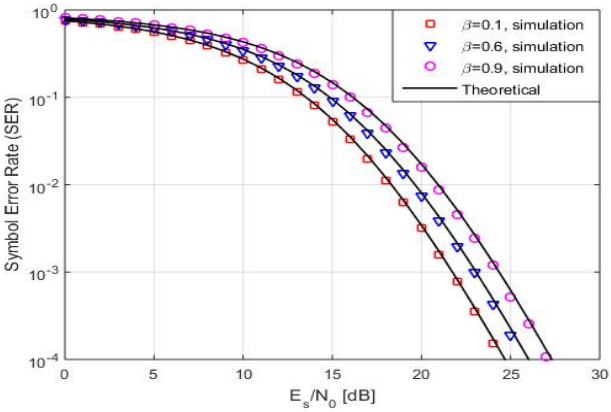

Fig. 5. SER vs E_S/N_o analysis for various Roll-off factors.

The SER analysis for various SNRs is plotted in Fig. 6 for several modulation schemes (QPSK (k=2) and 16-QAM (k=4)), N_t=1, and α=2 and μ=5. We may conclude from this simulation that the SER value for the QPSK technique is lower than 16-QAM modulation method. For a specific scenario, the SER values for the 16-QAM and QPSK methods are 0.0251 and 0.0072, respectively at SNR=10dB.

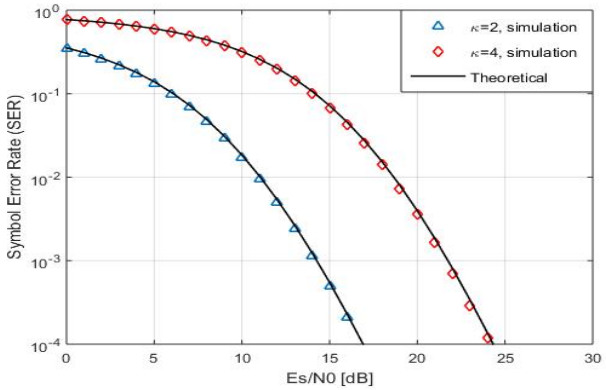

Fig. 6. SER vs E_s/N_o analysis for various modulation schemes.

5. Conclusion

The performance of SER is examined in this study using GFDM system under $\alpha-\mu$ fading. The novel closed form of SER expression under $\alpha-\mu$ fading environment was initially derived in this paper. Later, using MATLAB simulations for a variety of simulation parameters such fading parameters, various roll-off factors, and various modulation orders, the performance of the SER is assessed. We have used the

published literature studies to validate our simulations as well. We have observed that the error rate is dropped as one fading parameter was fixed and another fading parameter was increased. Additionally, the overall performance of the SER using GFDM system is significantly influenced by the roll-off factor selection also. The studied system model under $\alpha - \mu$ fading is useful in designing the wireless communication system in a more generalized manner.

References

[1] A. Farhang, N. Marchetti, and L. E. Doyle, "Low-Complexity Modem Design for GFDM," *IEEE Trans. Signal Process.*, vol. 64, no. 6, pp. 1507–1518, Mar. 2016, doi: 10.1109/TSP.2015.2502546.

[2] Z. Sharifian, M. J. Omidi, A. Farhang, and H. Saeedi-Sourck, "Polynomial-based compressing and iterative expanding for PAPR reduction in GFDM," in *2015 23rd Iranian Conf. Electr.l Engin.*, Tehran, Iran: IEEE, May 2015, pp. 518–523. doi: 10.1109/IranianCEE.2015.7146271.

[3] J. S. Ferreira *et al.*, "GFDM Frame Design for 5G Application Scenarios," *J. Communic. Inform. Sys.*, vol. 32, no. 1, pp. 54–61, 2017, doi: 10.14209/jcis.2017.6.

[4] D. Zhang, M. Matthe, L. L. Mendes, and G. Fettweis, "A Study on the Link Level Performance of Advanced Multicarrier Waveforms Under MIMO Wireless Communication Channels," *IEEE Trans. Wireless Commun.*, vol. 16, no. 4, pp. 2350–2365, Apr. 2017, doi: 10.1109/TWC.2017.2664820.

[5] N. Michailow *et al.*, "Generalized Frequency Division Multiplexing for 5th Generation Cellular Networks," *IEEE Trans. Commun.*, vol. 62, no. 9, pp. 3045–3061, Sep. 2014, doi: 10.1109/TCOMM.2014.2345566.

[6] N. Michailow, L. Mendes, M. Matthe, I. Gaspar, A. Festag, and G. Fettweis, "Robust WHT-GFDM for the Next Generation of Wireless Networks," *IEEE Commun. Lett.*, vol. 19, no. 1, pp. 106–109, Jan. 2015, doi: 10.1109/LCOMM.2014.2374181.

[7] I. Gaspar, L. Mendes, M. Matthe, N. Michailow, A. Festag, and G. Fettweis, "LTE-compatible 5G PHY based on generalized frequency division multiplexing," in *2014 11th Int. Symp. Wirel. Communic. Sys. (ISWCS)*, Barcelona, Spain: IEEE, Aug. 2014, pp. 209–213. doi: 10.1109/ISWCS.2014.6933348.

[8] G. Fettweis, M. Krondorf, and S. Bittner, "GFDM - Generalized Frequency Division Multiplexing," in *VTC Spring 2009 - IEEE 69th Vehicul. Techn. Conf.*, Barcelona, Spain: IEEE, Apr. 2009, pp. 1–4. doi: 10.1109/VETECS.2009.5073571.

[9] S. K. Antapurkar, A. Pandey, and K. K. Gupta, "GFDM performance in terms of BER, PAPR and OOB and comparison to OFDM system," *presented at the Adv. Sci. Technol.: Proceed. 2nd Int. Conf. Commun. Sys. (ICCS-2015),* Rajasthan, India, 2016, p. 020039. doi: 10.1063/1.4942721.

[10] A. Kumar and M. Magarini, "Improved Nyquist pulse shaping filters for generalized frequency division multiplexing," in *2016 8th IEEE Latin-American Conf. Communic. (LATINCOM)*, Medellin, Colombia: IEEE, Nov. 2016, pp. 1–7. doi: 10.1109/LATINCOM.2016.7811588.

[11] N. Michailow and G. Fettweis, "Low peak-to-average power ratio for next generation cellular systems with generalized frequency division multiplexing," in *2013 Int. Symp. Intellig. Sign. Process. Communic. Sys.*, Naha-shi, Japan: IEEE, Nov. 2013, pp. 651–655. doi: 10.1109/ISPACS.2013.6704629.

[12] S. K. Mishra and K. D. Kulat, "Approximation of peak-to-average power ratio of generalized frequency division multiplexing," *AEU – Int. J. Elec. Comm.*, vol. 99, pp. 247–257, Feb. 2019, doi: 10.1016/j.aeue.2018.12.001.

[13] S. G. Neelam and P. R. Sahu, "Error performance of QAM GFDM waveform with CFO under AWGN and TWDP fading channel," in *2019 Nat. Conf. Communic. (NCC)*, Bangalore, India: IEEE, Feb. 2019, pp. 1–6. doi: 10.1109/NCC.2019.8732207.

[14] M. Matthe, N. Michailow, I. Gaspar, and G. Fettweis, "Influence of pulse shaping on bit error rate performance and out of band radiation of Generalized Frequency Division Multiplexing," in *2014 IEEE Int. Conf. Commun. Worksh. (ICC)*, Australia: IEEE, Jun. 2014, pp. 43–48. doi: 10.1109/ICCW.2014.6881170.

[15] V. Nivetha and V. Sudha, "BER Analysis of GFDM System Under Different Pulse Shaping Filters," in *2021 Sixth Int. Conf. Wirel. Commun., Sign. Proc. Networ. (WiSPNET)*, Chennai, India: IEEE, Mar. 2021, pp. 53–56. doi: 10.1109/WiSPNET51692.2021.9419396.

[16] A. Nimr, M. Chafii, and G. Fettweis, *Practical GFDM-based Linear Receivers*. DE: VDE VERLAG GMBH, 2019. Accessed: Sep. 01, 2024. [Online]. Available: https://doi.org/10.30420/454862039

[17] M. Carrick and J. H. Reed, "Improved GFDM equalization in severe frequency selective fading," in *2017 IEEE 38th Sarnoff Symp.*, Newark, NJ, USA: IEEE, Sep. 2017, pp. 1–6. doi: 10.1109/SARNOF.2017.8080391.

[18] N. Michailow, S. Krone, M. Lentmaier, and G. Fettweis, "Bit Error Rate Performance of Generalized Frequency Division Multiplexing," in *2012 IEEE Vehicular Techn. Conf. (VTC Fall)*, Quebec City, QC, Canada: IEEE, Sep. 2012, pp. 1–5. doi: 10.1109/VTCFall.2012.6399305.

[19] R. Datta, N. Michailow, M. Lentmaier, and G. Fettweis, "GFDM Interference Cancellation for Flexible Cognitive Radio PHY Design," in *2012 IEEE Vehicular Techn. Conf (VTC Fall)*, Quebec City, QC: IEEE, Sep. 2012, pp. 1–5. doi: 10.1109/VTCFall.2012.6399031.

[20] S. Tiwari, S. Sekhar Das, and K. K. Bandyopadhyay, "Precoded generalised frequency division multiplexing system to combat inter-carrier interference: performance analysis," *IET Communic.*, vol. 9, no. 15, pp. 1829–1841, Oct. 2015, doi: 10.1049/iet-com.2015.0081.

[21] M. Matthe, L. L. Mendes and G. Fettweis, "Space-Time Coding for Generalized Frequency Division Multiplexing," *European Wireless 2014; 20th European Wireless Conf.*, Barcelona, Spain, May 2014, pp. 1-5.

[22] M. Matthe, L. L. Mendes, N. Michailow, D. Zhang, and G. Fettweis, "Widely Linear Estimation for Space-Time-Coded GFDM in Low-Latency Applications," *IEEE Trans. Commun.*, vol. 63, no. 11, pp. 4501–4509, Nov. 2015, doi: 10.1109/TCOMM.2015.2468228.

[23] J. Zhang, M. Matthaiou, Z. Tan, and H. Wang, "Performance Analysis of Digital Communication Systems Over Composite η-μ/gamma Fading Channels," *IEEE Trans. Veh. Technol.*, vol. 61, no. 7, pp. 3114–3124, Sep. 2012, doi: 10.1109/TVT.2012.2199344.

[24] C. Ben Issaid, M.-S. Alouini, and R. Tempone, "On the Fast and Precise Evaluation of the Outage Probability of Diversity Receivers Over α - μ , κ - μ , and η-μ fading Channels," *IEEE Trans. Wireless Commun.*, vol. 17, no. 2, pp. 1255–1268, Feb. 2018, doi: 10.1109/TWC.2017.2777465.

[25] B. Sklar, *Digital communications: fundamentals and applications*, 3rd ed. Hoboken: Pearson Education, Inc, 2020.

[26] M. D. Yacoub, "The $\alpha - \mu$ Distribution: A Physical Fading Model for the Stacy Distribution," *IEEE Trans. Veh. Technol.*, vol. 56, no. 1, pp. 27–34, Jan. 2007, doi: 10.1109/TVT.2006.883753.

[27] I. S. Gradshteĭn and D. Zwillinger, *Table of integrals, series, and products*, Eighth edition. Amsterdam ; Boston: Elsevier, Academic Press is an imprint of Elsevier, 2015.

[28] A. Yenilmez, T. Gucluoglu, and P. Remlein, "Performance of GFDM-maximal ratio transmission over Nakagami-m fading channels," in *2016 Int. Symp. Wirel. Communic. Sys. (ISWCS)*, Poznan, Poland: IEEE, Sep. 2016, pp. 523–527. doi: 10.1109/ISWCS.2016.7600960.

[29] S. K. Bandari, V. V. Mani, and A. Drosopoulos, "Performance analysis of GFDM in various fading channels," *COMPEL: The Int. J. Comput. Mathem. Electric. Electr. Engineer.*, vol. 35, no. 1, pp. 225–244, Jan. 2016, doi: 10.1108/COMPEL-06-2015-0215.

[30] L. Jada and S. Shiyamala, "Investigation on GFDM System for 5G Applications over Fading Channels," *J. Eng. Sci. Techn. Rev.*, vol. 15, no. 3, pp. 1–8, Feb. 2022, doi: 10.25103/jestr.153.01.